

Differently Shaped Hard Body Colloids in Confinement: From passive to active particles

H. H. Wensink¹, H. Löwen², M. Marechal³, A. Härtel⁴, R. Wittkowski⁵,
U. Zimmermann², A. Kaiser², and A. M. Menzel²

¹ Laboratoire de Physique des Solides, Université Paris-Sud and CNRS, 91405 Orsay, France

² Institut für Theoretische Physik II: Weiche Materie, Heinrich-Heine-Universität Düsseldorf, 40225 Düsseldorf, Germany

³ Institut für Theoretische Physik I, Universität Erlangen-Nürnberg, 91058 Erlangen, Germany

⁴ ITF, Utrecht University, MG 305, Leuvenlaan 4, 3584 CE Utrecht, The Netherlands

⁵ SUPA, School of Physics and Astronomy, University of Edinburgh, Edinburgh EH9 3JZ, United Kingdom

Abstract. We review recent progress in the theoretical description of anisotropic hard colloidal particles. The shapes considered range from rods and dumbbells to rounded cubes, polyhedra to biaxial particles with arbitrary shape. Our focus is on both static and dynamical density functional theory and on computer simulations. We describe recent results for the structure, dynamics and phase behaviour in the bulk and in various confining geometries, e.g. established by two parallel walls which reduce the dimensionality of the system to two dimensions. We also include recent theoretical modelling for active particles, which are autonomously driven by some intrinsic motor, and highlight their fascinating nonequilibrium dynamics and collective behaviour.

1 Introduction

Nowadays anisotropic colloidal particles can be prepared in a controlled way and almost any shape can be realized [1,2,3]. In their simplest form, the particles are sterically stabilized so that their interactions can be described by excluded volume alone. This implies that temperature scales out (the thermal energy $k_B T$ trivially sets the energy scale) such that in the bulk the density (or the packing fraction) is the only relevant thermodynamic parameter. In the absence of external fields, the dynamics of a colloidal particle is Brownian due to random forces exerted by the solvent molecules. The additional degree of anisotropy has given a boost to the development of new statistical theories for anisotropic particles and extended methods for computer simulations. For example, the traditional theory of Brownian motion has been widely applied to spherical and rod-like particles with a rotational symmetry [4,5]. Case studies of particles with an arbitrary shape have not yet been fully considered in theory and simulation, although the theoretical principles date back to 1934 when Perrin [6] developed the basic ideas. Density functional theory is typically formulated

for systems of spherical particles whereas generalized theories appropriate for systems with orientational degrees of freedom are scarce.

A system of hard nonspherical particles can be exposed to an external confinement, which leads to even more complex behaviour, see the complexity diagram in [7]. The simplest types of confinement are an external planar hard wall (see e.g. [8,9]), two parallel hard plates (“slit geometry”) [10], or a templated wall [11]. Other options are periodic modulations induced by a laser field (so called optical gratings) [12,13], which are found to induce highly non-trivial phase behaviour for simple spheres [14,15,16,17,18,19,20,21]. The extreme limit of a slit geometry is a complete reduction in dimensionality down to two spatial dimensions. The same reduction can be achieved if colloids are confined to interfaces [22,23]. In general, confinement brings in additional system parameters which require a more generic statistical theory to describe inhomogeneous systems.

In contrast to passive particles, self-propelled particles dissipate energy and exhibit autonomous, directed motion. This leads to intrinsic nonequilibrium behaviour [24,25,26]. The self propulsion specifies a direction in orientational phase space, which renders active particles and their interactions inherently anisotropic, even though their shape might be spherical. Several varieties of self-propelled colloidal particles have been prepared in which external fields play a leading role in the self-propagation mechanism. Prominent examples include catalytically driven Janus particles [27] and thermally driven colloids in a phase-separating solvent [28,29,30]. Last but not least, autonomously moving bacteria (such as *Bacillus subtilis*) exhibit characteristics similar to self-propelled colloidal particles [31].

In this paper, we review recent progress in the theoretical description of anisotropic hard colloidal particles. The various shapes considered range from simple rods and dumbbells to rounded cubes, polyhedra and to particles with arbitrary biaxiality. Here we mainly use static and dynamical density functional theory and we test the theory against computer simulations. We describe recent results for the structure, dynamics and phase behaviour in bulk and in various confining geometries. We also include results from recent theoretical modelling of ensembles of active particles and highlight the main features of their collective behaviour.

The review is organized as follows: in sec. 2 we present a general overview of results from density functional theory, both static and dynamical, for anisotropic particles before discussing some explicit results obtained from fundamental-measure theory for rods [32,33], dumbbells [34], rounded cubes [35], and regular polyhedra [36] in sec. 3. In sec. 4, we turn to Brownian dynamics of anisotropic particles, both in equilibrium and nonequilibrium situations. Section 5 is devoted to single-particle and collective behaviour of self-propelled colloids and we conclude in sec. 6.

2 Density functional theory

2.1 Static density functional theory: Fundamental-measure theory

Classical density functional theory of freezing [37,38,39,40,41] provides an ideal framework to describe nonuniform fluids. Confinement can be studied in a very elegant way, because an external potential enters very naturally in the theoretical framework. One of the most successful approximations for the hard sphere functional is based on the fundamental-measure theory (FMT) of Rosenfeld [42] (see [43] for a review), which is purely geometry-based. This theory has been extended to colloid-polymer mixtures [44](see [21] for an application). More importantly, it has been generalized towards hard particles with arbitrary shape (for related work see [45,46]) by Hansen-Goos and Mecke [47,48] who have extended the FMT framework by including the

orientational degrees of freedom of biaxial particles [2]. In the extended fundamental-measure theory (henceforth referred to as E-FMT) the one-body density depends on the centre-of-mass position and orientation while particle interactions are assumed to be hard.

Although the E-FMT provides a general framework to study a vast repertoire of particle shapes, only the case of hard spherocylinders in the fluid phase was considered in the original paper [47]. Recent efforts have focussed on testing the applicability of E-FMT for other particle shapes such as dumbbells [34], rounded cubes [35] and regular polyhedra [36]. We summarize these situations in the following sections.

2.2 Dynamical density functional theory for biaxial particles

On large timescales colloidal particles exhibit completely overdamped Brownian dynamics due to solvent friction. For spherical Brownian particles, dynamical density functional theory (DDFT) was derived by either starting from the Langevin equations [49], the Smoluchowski equation [50], or the Mori-Zwanzig projection operator technique [51](see [52] for a recent review). Subsequently, a DDFT for uniaxial anisometric particles [53] has been set up based on the Smoluchowski-based approach proposed in [50]. The case of uniaxial particles involves three friction (or mobility) coefficients, namely the translational friction parallel and perpendicular to the main particle orientation and the rotational friction.

More recently, DDFT has been extended to rigid biaxial particles with an arbitrary shape [2]. In these situations the friction matrix is much more complicated due to various nontrivial translational-rotational couplings. This is important for, e.g. screw-shaped particles where an imposed translational movement induces rotational motion and vice versa.

2.3 Phase-field-crystal models for liquid crystals

In density functional theory (DFT), the one-particle density depends on the centre-of-mass position and on the orientation. For uniaxial particles, the orientational dependence can be expanded into spherical harmonics such that the density is parametrized with just position-dependent order-parameter fields such as the mean density, polarization, and nematic order [52,54]. Using an order-parameter gradient expansion [55,56,57,58], one can use DDFT as a starting point to derive simpler theories for the dynamics of liquid crystals. For spheres, these class of theories are usually referred to as phase-field-crystal (PFC) models as originally introduced in 2002 by Elder and coworkers [59](see [52] for a review). PFC theory is capable of predicting a vast range of phase transitions to positionally ordered structures commonly observed in hard and soft condensed matter. A generalized PFC model for systems with orientational degrees of freedom has been recently developed in both two [60] and three [54] spatial dimensions. The simplified theory is still microscopic in the sense that the PFC coupling parameters can be related to various microscopic properties of the system such as the pair potential and pair correlation function. As such the extended PFC model provides an approximate yet microscopically founded framework for the calculation of phase diagrams of liquid crystals [61]. Moreover, it can be used as a useful starting point for addressing dynamical processes of anisotropic particles since the PFC models are technically less demanding than their DDFT counterparts.

3 Passive colloids: statics

3.1 Hard spherocylinders

The phase diagram of spherocylinders has been computed by Bolhuis and Frenkel [62] and features stable isotropic, nematic, smectic A phases, as well as plastic and orientationally-ordered *AAA* or *ABC* stacked crystals. The work of Bolhuis and Frenkel [62] thus provides excellent benchmark data to test density functional theories for rodlike colloids [63]. The recently developed E-FMT has been applied to inhomogeneous isotropic and nematic phases [32] but the computation of the full phase diagram is still hampered by the enormous numerical effort required to evaluate the functional for structured phases such as smectic A and plastic crystal. Preliminary calculations, however, seem to indicate that there is no stable smectic A phase [64]. This result clearly contradicts observations from simulation and experiment and thus prompts a careful study of the numerical implementation of E-FMT. It would also be interesting to address the plastic-crystalline state. In particular, one could explore the nontrivial topology of the director field inside a unit cell which has recently been unveiled using computer simulations [33].

The numerical burden can be significantly reduced by applying E-FMT to spherocylinders in strong aligning fields which only couple to the orientational degrees of freedom [63]. Numerical results for the isotropic and nematic fluids of spherocylinders and their coexistence are presented in [32].

3.2 Hard dumbbells

A hard dumbbell consists of two fused hard spheres of diameter σ whose centres are separated by a distance $L < \sigma$. Note that this produces a nonconvex shape. Different synthesis methods have been successfully applied to prepare colloidal dumbbells [65,66,67]. Samples of colloidal dumbbells have been used to study bulk crystallization [68] and quasi two-dimensional degenerate crystals [67,69,70]. Moreover, the bulk phase behaviour of hard dumbbells is well-known from simulations [71,72,73,74,75].

In the recent work [34], E-FMT was applied to an inhomogeneous fluid of hard dumbbells. For various values of L/σ and varied particle concentration, density profiles for dumbbells in a slit-geometry were computed and found to be in good agreement with simulations for bulk packing fractions η up to about 0.3. An example is shown in Fig. 1.

DFT is also an ideal tool to explore sedimentation profiles [76]. Therefore, density profiles of dumbbells in a gravitational field were computed and compared to simulations [77]. Again reasonable agreement was found between simulation and DFT. This shows that the E-FMT [47,48] gives an accurate prediction of the structure of hard particles with a nonconvex shape at low to moderate particle density. Deviations between theory and simulation appear at higher packing fractions. These results suggest that the applicability of E-FMT is limited to particle shapes that do not deviate too much from spherical particles.

3.3 Hard rounded cubes

In the recent pioneering work of Rossi et al. [78], well-defined colloidal cubes were prepared and studied in real space by confocal microscopy. These cubes typically possess rounded edges, motivating a modelling by a hard “spherocube” with rounded edges of outer curvature diameter d and an inner cubic part of edge length σ (see

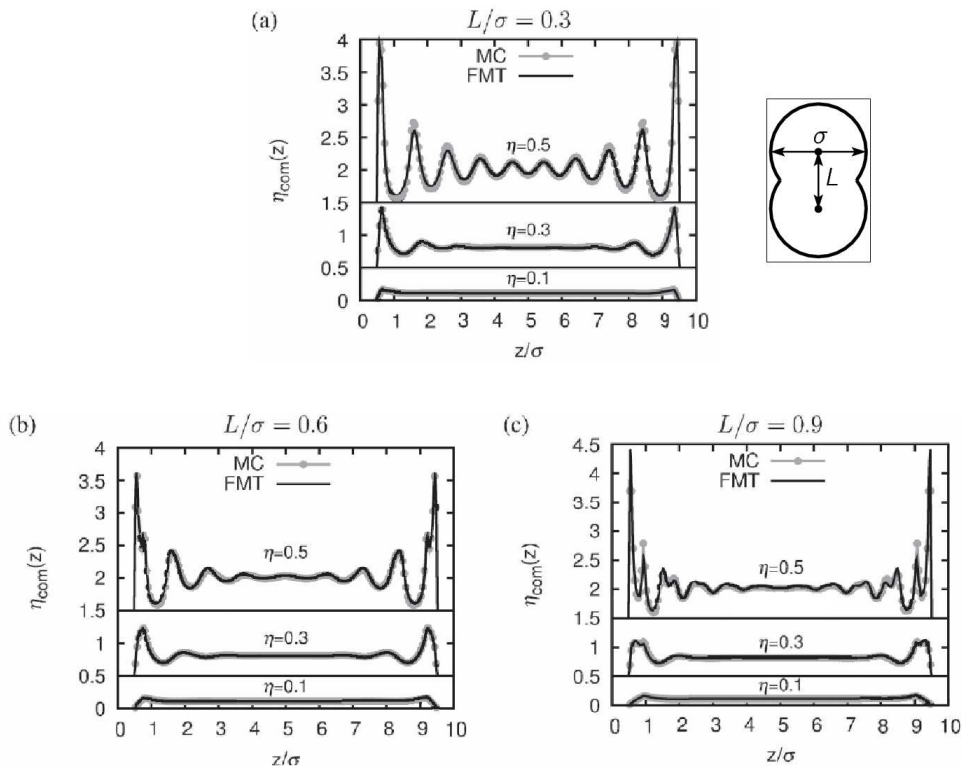


Fig. 1: The centre-of-mass density profile $\eta_{\text{com}}(z)$, in units of the volume of a dumbbell, as a function of the height z between two parallel walls for dumbbells of diameter σ and three different values of L/σ at bulk volume fractions η . Monte-Carlo simulation results are denoted by the gray dots and the FMT results by the black line. From [34].

Fig. 2 for a sketch). Colloidal cubes can in principle be oriented by external aligning fields [79,80], for instance by introducing an inner core with two distinct nonparallel dipole moments, each of which couples to a separate external field. Considering perfectly aligned cubes greatly facilitates the theoretical analysis, since the orientational degrees of freedom of the cubes do not play a role.

The bulk phase diagram of parallel hard spherocubes was recently derived from simulations [35] and the results are shown in Fig. 3 as a function of the rounding parameter $s = d/\ell$ and the cube packing fraction η . The special case $s = 0$ of parallel cubes was studied earlier by Cuesta and coworkers [81,82,83,84] and a second-order freezing transition into a simple cubic lattice was found. Second-order freezing is quite unusual in three dimensions and is intimately linked to the (cubic) anisotropy of the fluid phase along with the properties of the simple cubic solid. A second-order freezing transition occurs over a broad range of $s > 0$ (see Fig. 3). E-FMT calculations confirm the second-order character of the phase transition and give a transition packing fraction η in good agreement with the simulation values, as evident from Fig. 3. Moreover, the simulations predict new crystal structures at larger values of s and high density corresponding to a sheared cubic lattice and a deformed face-centred-cubic (fcc) lattice which occurs in two variants: *ortho* and *clino*. We emphasize that the present phase diagram is completely different from that of freely oriented hard

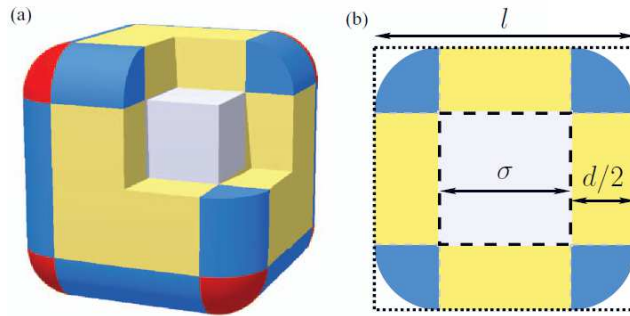


Fig. 2: (a) A spherocube or rounded cube consists of a cube (lightest/gray) surrounded by 6 square prisms (darker/yellow), 12 cylinder sections (still darker/light blue), and 8 spherical sections (darkest/red). Some sections of the outer objects have been removed to show the gray cube. (b) Cross section of the spherocube showing the edge length σ , minimum radius of curvature $d/2$ and the total width ℓ . From [35].

cubes which exhibit a first-order freezing transition and vacancy-stabilized crystalline order [85]. The case of hard squares in two spatial dimensions has been studied by Belli and coworkers [86].

3.4 Hard polyhedra

The close-packed configuration of polyhedra, in particular tetrahedra [87,88,89,90], has been intensely discussed as of late [91,92]. At intermediate densities novel states show up [93,94], such as an emergent quasicrystalline state for hard tetrahedra [95]. Regarding theory for hard polyhedra there are some equation-of-state predictions (see [36] for a discussion), but a microscopic theory for inhomogeneous systems has not been analyzed.

In order to fill this gap, the E-FMT [47,48] has recently been applied to the layering of orientable hard polyhedral fluids near a hard wall [36]. Density profiles for fluids of hard tetrahedra, cubes, octahedra and dodecahedra near a hard wall are shown in Fig. 4. There is reasonable agreement with simulation data, although the agreement deteriorates for low-order polyhedra (like tetrahedra). The fact that highly regular polyhedra, whose shapes closely resemble that of a sphere, can be accurately described by E-FMT underlines the notion that the theory is optimized for (near-)spherical objects. The density profiles plotted as a function of the centre-of-mass position, exhibit characteristic peaks which correspond to special configurations of a single polyhedron close to a planar wall. The corresponding orientations are also depicted in Fig. 4.

4 Passive colloids: dynamics

4.1 Brownian dynamics of biaxial particles

In three spatial dimensions, the Brownian motion of colloidal particles with arbitrary shape involves a hydrodynamic coupling between the translational and the rotational degrees of freedom, which was described theoretically, for example, by Brenner [96,97]. In 2002, Fernandes and Garcia de la Torre [98] proposed a corresponding Brownian dynamics simulation algorithm for the motion of a passive rigid particle with arbitrary

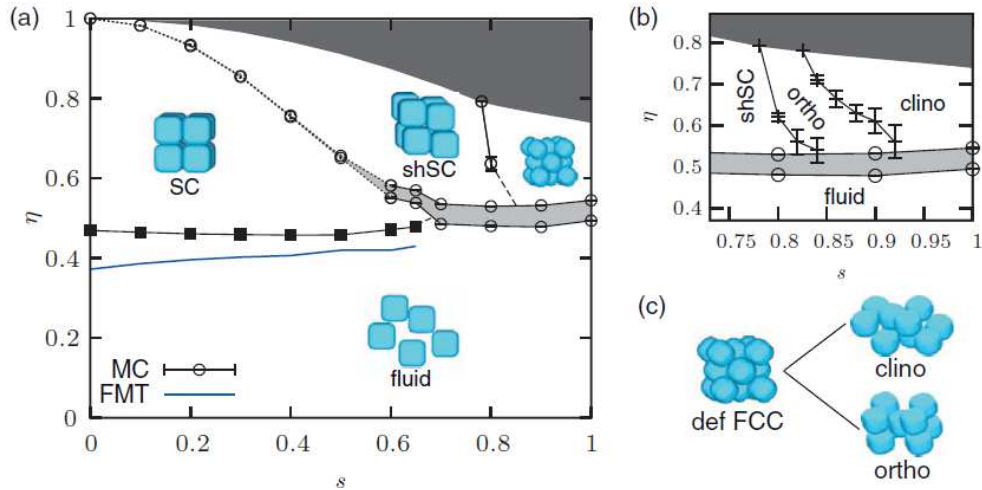


Fig. 3: (a) Phase diagram of parallel rounded cubes in the s - η representation, where η is the packing fraction and $s = d/\ell$ is the rounding parameter (see Fig. 2). A cube corresponds to $s = 0$ and a sphere to $s = 1$. Shown are the areas of stability of the deformed fcc phase of near spheres (def FCC), the sheared cubic crystal (shSC), the simple cubic crystal (SC), and the fluid phase in white. The forbidden region above the close packing density is shown in dark gray and coexistence areas in lighter gray (coexistence lines are vertical). The filled symbols (MC simulations) and the thick line (FMT) denote second-order phase transitions, while the empty symbols denote first-order phase transitions from simulations. (b) Enlarged view of the large- s region of the phase diagram: the def FCC phase is actually seen to have a body-centred orthorhombic variant (ortho) and a base-centred monoclinic variant (clino), as depicted in (c). From [35].

shape. The underlying equations of motion were generalized towards an imposed external flow field for the surrounding fluid by Makino and Doi [99]. Only recently, the full expression for the Langevin equations in Ito formalism including the drift term was derived in [100], for the stochastically equivalent Smoluchowski formalism see [2]. The predicted Brownian trajectories were experimentally confirmed [101].

4.2 Nonequilibrium dynamics in time-dependent external fields

DDFT based on fundamental-measure theory for anisotropic particles has recently been employed in two cases concerning isotropic and nematic fluids of hard spherocylinders in time-dependent aligning fields. First, the relaxational behaviour following an instantaneous switch in the direction of the aligning field was analyzed in [32], which complements an earlier study considering a time-dependent translational confinement of soft rods [53]. Second, an anisotropic fluid was subject to an aligning field rotating at a constant angular speed. The nonequilibrium response of the system involves a number of novel nonequilibrium steady states in the time-dependent orientational distribution [102].

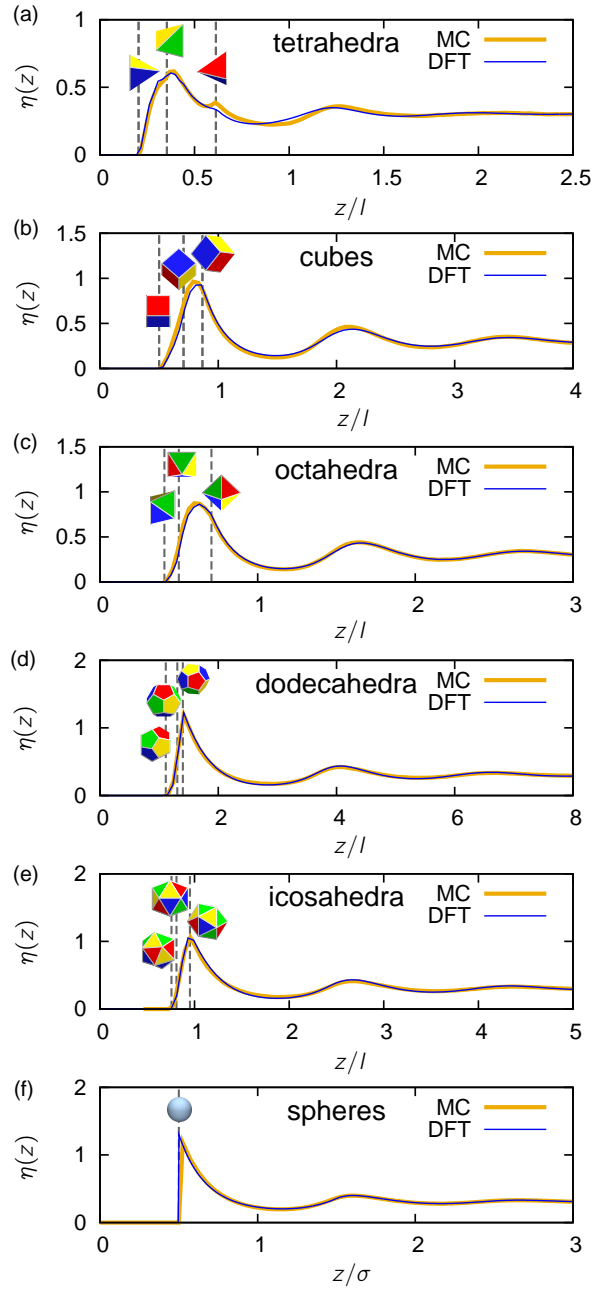


Fig. 4: Centre-of-mass density profiles $\eta(z)$ as a function of the height z divided by the edge length ℓ for one-component systems of (a) tetrahedra, (b) cubes, (c) octahedra, (d) dodecahedra and (e) icosahedra near a hard wall located at $z = 0$. Fundamental measure density functional theory (DFT; dark, blue curves) is compared to results from Monte-Carlo simulations (MC; light, orange curves). The average volume fraction is set to $\eta = 0.3$. (f) The density profile of spheres for the same packing fraction $\eta = 0.3$ is shown as a function of z divided by the sphere diameter σ for comparison. The heights z for which a particle can just touch the wall with a vertex, an edge and a face are indicated by the dashed lines; also shown are polyhedra with the corresponding orientations. From [36].

5 Active colloids

5.1 Trajectories of a single self-propelled particle

The simplest model for a single self-propelled (active) colloidal particle is a Brownian particle with an *internal* drive, i.e. with a propagation along an inner degree of freedom as modelled by an intrinsic “force” and “torque”. In the absence of thermal noise the trajectories are closed circles in two spatial dimensions [103,104] but much more complex trajectories arise in three spatial dimensions [100]. In particular the trajectories of orthotropic particles, which have no translational-orientational coupling in the hydrodynamic friction matrix, are helices. In general, the translational-rotational coupling of the hydrodynamic friction, however, leads to more complicated trajectories which have been classified in [100]. The coupling to the thermal Brownian motion yields nontrivial behaviour for the mean-square displacement, which can be worked out analytically for a constant intrinsic drive [105] and a uniaxial particle. For a biaxial particle the problem becomes too complex and the average particle trajectories can only be assessed numerically [100]. In two dimensions, the trajectory statistics were confirmed in experiments [29].

Finally, we mention the motion of self-propelled particles in gradient fields of a chemical [106]. In a poison field that weakens the drive, nontrivial scaling behaviour for the mean-square displacement has been obtained in [107] while the dynamics of a chemotactic predator-prey model has been explored in [108].

5.2 Collective properties of self-propelled rod-like particles

The competition between the intrinsic self-propulsion and the interparticle interactions yields novel emerging behaviour for dense systems of self-propelled colloids. Particle-resolved colloidal models consisting of self-propelled rods (SPR) interacting via a soft but strongly screened Yukawa potential have become standard and can be simulated with and without Brownian noise [109]. In fact, these types of segment models have been routinely used to describe fluids of charged rods in thermal equilibrium [110,111]. Recently, these models have proven very useful in describing collective bacterial motion in *Bacillus subtilis* and *Escherichia coli* which have an effective aspect ratio of about 6 and 2, respectively [31]. At higher aspect ratios, self-propelled rods show a marked clustering in channel confinement, a phenomenon which is not encountered for passive rods in thermal equilibrium [109,112].

In bulk situations the noiseless SPR model exhibits a wealth of different steady states [113,31]. These are summarized in Fig. 5 in a state diagram spanned by the rod aspect ratio and the rod density. The reduced strength of the drive is fixed. Using suitable order parameters, such as the vorticity of a coarse-grained velocity field, one can discern various emergent states: from a disordered one in weakly interacting systems to a swarming state, a jammed state, and a laning state at higher density and aspect ratios. Most notably there is an intermediate turbulent (or bio-nematic) state (Fig. 5) which is distinguished from the swarming state by a significant occurrence of velocity swirls. The topology of the phase diagram was confirmed by experiments on strongly confined *Bacillus subtilis* suspensions [31]. The velocity correlations and energy spectrum in the turbulent flow do not follow the traditional Kolmogorov-Kraichnan scaling laws [31] which hints to a novel turbulent state in living fluids. In addition to linearly propagating rods, “circle swimmers” experience an additional active torque which may give rise to active self-assembly into vortex arrays [114].

Next, the question of how to efficiently capture many self-propelled rods near fixed boundaries was studied in [115]. It was shown that a wedge-like trap with

an appropriate opening angle constitutes an efficient trapping device for SPRs. The trapping efficiency has been classified in terms of a nonequilibrium phase diagram as a function of the wedge opening angle, the particle density and the trap density [115]. This diagram is shown in Fig. 6 and highlights three possible final states of no trapping at all, partial trapping and complete trapping in which situation all particles finally end up in the trap. We emphasise that the transition from partial to complete trapping is not a trivial consequence of the change in the (triangular) trap area. If the phase diagram were drawn at constant trap area, all three states would persist. The trapping behaviour was also recently generalized towards a moving net [116].

5.3 Active crystals

“Active” crystallization of self-propelled colloids was explored by means of particle-resolved computer simulations [117]. Possibilities to explore “active” crystallization within microscopic PFC models and DDFT were reported in [2]. It turned out that the bulk freezing transition in active systems occurs at much lower temperatures than in thermally equilibrated passive systems. Furthermore, at higher active drives or for spontaneous ordering of the self-propulsion directions, the crystal is predicted to propagate as a whole (“traveling crystal”) [118]. Clearly, experiments on colloidal swimmers are called for to confirm these predictions.

6 Conclusions

As documented by many applications, fundamental-measure density functional theory is a powerful predictive tool to describe the structure and dynamics of hard anisotropic particles. Dynamical density functional theory (DDFT) provides a viable starting framework for developing a microscopic theory for active colloidal particles, which show fascinating collective behaviour like swarming, laning, turbulence and “active” crystallization.

We finalise by outlining some unsolved problems which are interesting for future studies. While there has been considerable progress in reformulating DFT for fluids in porous media [119,120], the corresponding dynamical extension has not been explored thus far. Future work should also consider mixtures of anisotropic particles (like rod-platelet mixtures, polydisperse systems) which are highly relevant to many colloidal systems in nature. Mixing different shapes may lead to a wealth of new phase behaviours. Moreover, a DDFT with hydrodynamic interactions has been developed for spheres [121] but its extension to uniaxial and biaxial particles remains elusive. Finally, there is a keen interest to explore the dynamical response of anisometric particles in time-dependent confinement such as “breathing” traps [122].

This work was supported by the DFG within SFB TR6 (project D3).

References

1. A. IVLEV, H. LÖWEN, G. MORFILL, and C. P. ROYALL, *Complex Plasmas and Colloidal Dispersions: Particle-Resolved Studies of Classical Liquids and Solids*, Series in Soft Condensed Matter, World Scientific, 2012.
2. R. WITTKOWSKI and H. LÖWEN, *Molecular Physics* **109**, 2935 (2011).
3. S. C. GLOTZER and M. J. SOLOMON, *Nature Mater.* **6**, 557 (2007).
4. J. K. G. DHONT, *An Introduction to the Dynamics of Colloids*, Elsevier, 2003.

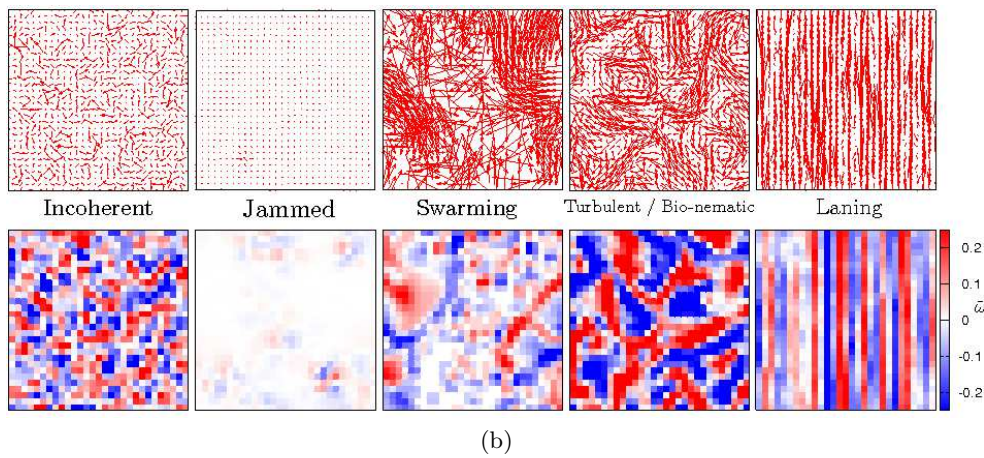
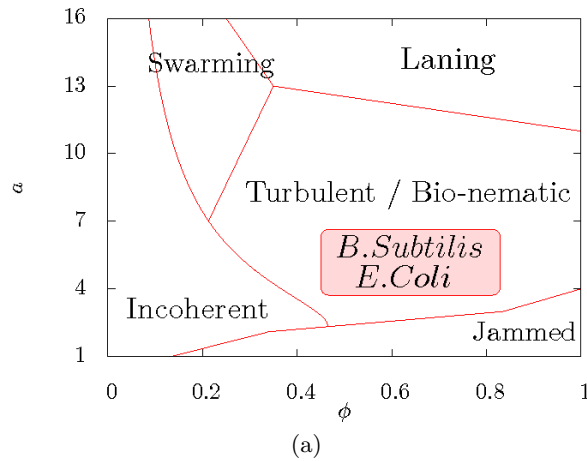


Fig. 5: (a) Schematic nonequilibrium phase diagram of self-propelled rods in two spatial dimensions with a variable aspect ratio a and effective filling fraction ϕ . Values exceeding unity are, in principle, possible due to the softness of the Yukawa interactions. The area relevant to self-motile bacteria is highlighted in red. (b) A number of distinctly different dynamical states are discernible as indicated by the coarse-grained maps of the velocity field (upper panels) and the corresponding scalar vorticity field in the steady state (lower panels). From [113].

5. H. LÖWEN, *Phys. Rev. E* **50**, 1232 (1994).
6. PERRIN, F., *J. Phys. Radium* **5**, 497 (1934).
7. H. LÖWEN, *J. Phys.: Condens. Matter* **13**, R415 (2001).
8. R. P. A. DULLENS, D. G. A. L. AARTS, and W. K. KEGEL, *Phys. Rev. Lett.* **97**, 228301 (2006).
9. K. SANDOMIRSKI, E. ALLAHYAROV, H. LÖWEN, and S. U. EGELHAAF, *Soft Matter* **7**, 8050 (2011).
10. S. NESER, C. BECHINGER, P. LEIDERER, and T. PALBERG, *Phys. Rev. Lett.* **79**, 2348 (1997).
11. J. P. HOOGENBOOM, A. K. VAN LANGEN-SUURLING, J. ROMIJN, and A. VAN BLAADEREN, *Phys. Rev. Lett.* **90**, 138301 (2003).
12. R. D. L. HANES, C. DALLE-FERRIER, M. SCHMIEDEBERG, M. C. JENKINS, and S. U. EGELHAAF, *Soft Matter* **8**, 2714 (2012).

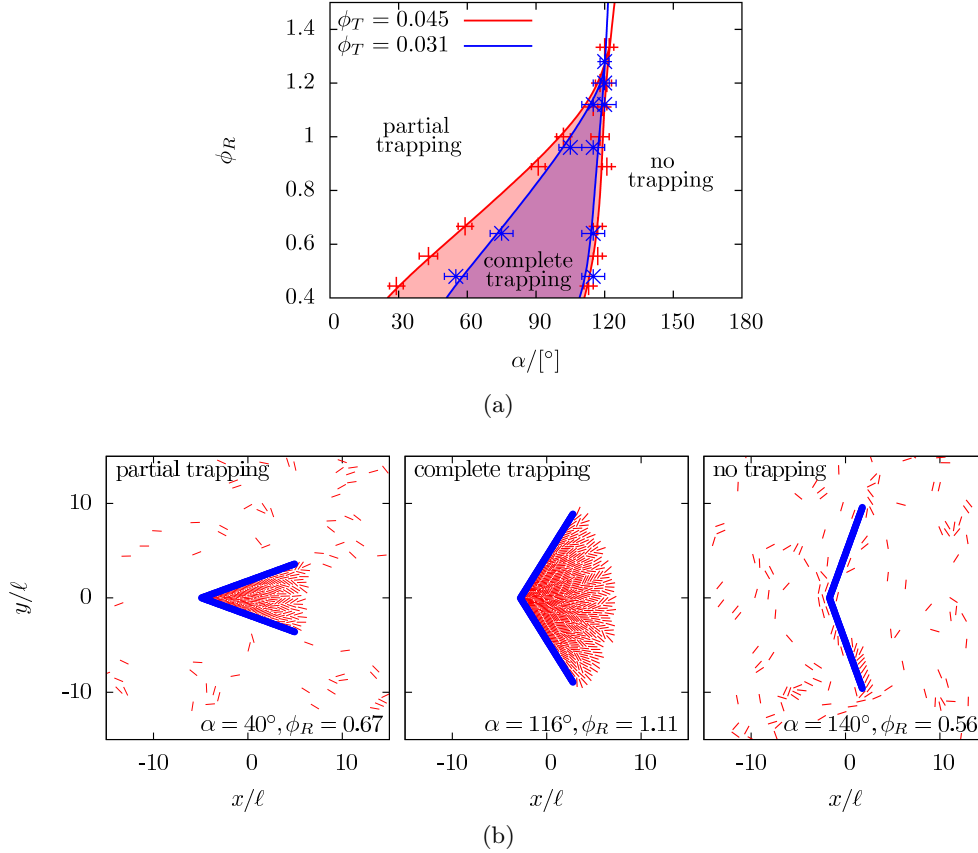


Fig. 6: (a) Nonequilibrium phase diagram marking three different collective trapping states of SPRs at a chevron boundary with total length of 20 rod lengths ℓ ; no trapping at large apex angle α , complete trapping at medium α and partial trapping at small α upon variation of the reduced rod packing fraction $\phi_R = \phi/\phi_T$. Phase boundaries are shown for two different values of the area fraction ϕ_T occupied by the (periodically repeated) traps. The region of complete trapping is bounded by a triple point at larger rod concentration beyond which a smooth transition from no trapping to partial trapping occurs. (b) Computer simulation snapshots showing stationary configurations of the three different states. From [115].

13. F. EVERS, R. D. L. HANES, C. ZUNKE, R. F. CAPELLMANN, J. BEWERUNGE, C. DALLE-FERRIER, M. C. JENKINS, I. LADADWA, A. HEUER, R. CASTAÑEDA PRIEGO, and S. U. EGELHAAF, *submitted to Eur. Phys. J. Special Topics*.
14. H. H. WENSINK and R. L. C. VINK, *J. Phys.: Condens. Matter* **19**, 466109 (2007).
15. H. H. WENSINK, *J. Chem. Phys.* **126**, 194901 (2007).
16. A. D. VIRGILIS, R. L. C. VINK, J. HORBACH, and K. BINDER, *Europhys. Lett.* **77**, 60002 (2007).
17. R. L. C. VINK, *Phys. Rev. Lett.* **98**, 217801 (2007).
18. J. M. BRADER and R. L. C. VINK, *J. Phys.: Condens. Matter* **19**, 036101 (2007).
19. C. P. ROYALL, J. DZUBIELLA, M. SCHMIDT, and A. VAN BLAADEREN, *Phys. Rev. Lett.* **98**, 188304 (2007).

20. D. VAN DER BEEK, H. REICH, P. VAN DER SCHOOT, M. DIJKSTRA, T. SCHILLING, R. VINK, M. SCHMIDT, R. VAN ROIJ, and H. N. W. LEKKERKERKER, *Phys. Rev. Lett.* **97**, 087801 (2006).
21. R. L. C. VINK, T. NEUHAUS, and H. LÖWEN, *J. Chem. Phys.* **134**, 204907 (2011).
22. P. DILLMANN, G. MARET, and P. KEIM, *submitted to Eur. Phys. J. Special Topics*.
23. J. BLEIBEL, A. DOMÍNGUEZ, and M. OETTEL, *submitted to Eur. Phys. J. Special Topics*.
24. P. ROMANCZUK, M. BÄR, W. EBELING, B. LINDNER, and L. SCHIMANSKY-GEIER, *Eur. Phys. J. Special Topics* **202**, 1 (2012).
25. M. E. CATES, *Rep. Prog. Phys.* **75**, 042601 (2012).
26. M. C. MARCHETTI, J.-F. JOANNY, S. RAMASWAMY, T. B. LIVERPOOL, J. PROST, R. MADAN RAO, and R. ADITI SIMHA, *submitted to Rev. Mod. Phys.* (2012).
27. A. ERBE, M. ZIENTARA, L. BARABAN, C. KREIDLER, and P. LEIDERER, *J. Phys.: Condens. Matter* **20**, 404215 (2008).
28. G. VOLPE, I. BUTTINONI, D. VOGT, H.-J. KÜMMERER, and C. BECHINGER, *Soft Matter* **7**, 8810 (2011).
29. F. KÜMMEL, B. TEN HAGEN, R. WITTKOWSKI, I. BUTTINONI, R. EICHHORN, G. VOLPE, H. LÖWEN, and C. BECHINGER, *Phys. Rev. Lett.* **110**, 198302 (2013).
30. I. BUTTINONI, J. BIALKÉ, F. KÜMMEL, H. LÖWEN, C. BECHINGER, and T. SPECK, *Phys. Rev. Lett.* **110**, 238301 (2013).
31. H. H. WENSINK, J. DUNKEL, S. HEIDENREICH, K. DRESCHER, R. E. GOLDSTEIN, H. LÖWEN, and J. M. YEOMANS, *Proc. Natl. Acad. Sci. USA* **109**, 14308 (2012).
32. A. HÄRTEL and H. LÖWEN, *J. Phys.: Condens. Matter* **22**, 104112 (2010).
33. P. CREMER, M. MARECHAL, and H. LÖWEN, *Europhys. Lett.* **99**, 38005 (2012).
34. M. MARECHAL, H. H. GOETZKE, A. HÄRTEL, and H. LÖWEN, *J. Chem. Phys.* **135**, 234510 (2011).
35. M. MARECHAL, U. ZIMMERMANN, and H. LÖWEN, *J. Chem. Phys.* **136**, 144506 (2012).
36. M. MARECHAL and H. LÖWEN, *Phys. Rev. Lett.* **110**, 137801 (2013).
37. R. EVANS, *Advances in Physics* **28**, 143 (1979).
38. Y. SINGH, *Physics Reports* **207**, 351 (1991).
39. H. LÖWEN, *Phys. Rep.* **237**, 249 (1994).
40. P. TARAZONA, J. CUESTA, and Y. MARTÍNEZ-RATÓN, Density Functional Theories of Hard Particle Systems, in *Theory and Simulation of Hard-Sphere Fluids and Related Systems*, edited by Á. MULERO, volume 753 of *Lecture Notes in Physics*, pp. 247–341, Springer Berlin Heidelberg, 2008.
41. J. WU and Z. LI, *Annual Review of Physical Chemistry* **58**, 85 (2007).
42. Y. ROSENFELD, *Phys. Rev. Lett.* **63**, 980 (1989).
43. R. ROTH, *J. Phys.: Condens. Matter* **22**, 063102 (2010).
44. M. SCHMIDT, H. LÖWEN, J. M. BRADER, and R. EVANS, *J. Phys.: Condens. Matter* **14**, 9353 (2002).
45. A. CHAMOIX and A. PERERA, *J. Chem. Phys.* **104**, 1493 (1996).
46. S. KORDEN, *Phys. Rev. E* **85**, 041150 (2012).
47. H. HANSEN-GOOS and K. MECKE, *Phys. Rev. Lett.* **102**, 018302 (2009).
48. H. HANSEN-GOOS and K. MECKE, *J. Phys.: Condens. Matter* **22**, 364107 (2010).
49. U. M. B. MARCONI and P. TARAZONA, *J. Phys.: Condens. Matter* **12**, A413 (2000).
50. A. J. ARCHER and R. EVANS, *J. Chem. Phys.* **121**, 4246 (2004).
51. P. ESPAÑOL and H. LÖWEN, *J. Chem. Phys.* **131**, 244101 (2009).
52. H. EMMERICH, H. LÖWEN, R. WITTKOWSKI, T. GRUHN, G. I. TÓTH, G. TEGZE, and L. GRÁNÁSY, *Advances in Physics* **61**, 665 (2012).
53. M. REX, H. H. WENSINK, and H. LÖWEN, *Phys. Rev. E* **76**, 021403 (2007).
54. R. WITTKOWSKI, H. LÖWEN, and H. R. BRAND, *Phys. Rev. E* **82**, 031708 (2010).
55. H. LÖWEN, T. BEIER, and H. WAGNER, *Europhys. Lett.* **9**, 791 (1989).
56. J. F. LUTSKO, *J. Chem. Phys.* **134**, 164501 (2011).
57. K. R. ELDER, N. PROVATAS, J. BERRY, P. STEFANOVIC, and M. GRANT, *Phys. Rev. B* **75**, 064107 (2007).

58. S. VAN TEEFFELLEN, R. BACKOFEN, A. VOIGT, and H. LÖWEN, *Phys. Rev. E* **79**, 051404 (2009).
59. K. R. ELDER, M. KATAKOWSKI, M. HAATAJA, and M. GRANT, *Phys. Rev. Lett.* **88**, 245701 (2002).
60. H. LÖWEN, *J. Phys.: Condens. Matter* **22**, 364105 (2010).
61. C. V. ACHIM, R. WITTKOWSKI, and H. LÖWEN, *Phys. Rev. E* **83**, 061712 (2011).
62. P. BOLHUIS and D. FRENKEL, *J. Chem. Phys.* **106**, 666 (1997).
63. H. GRAF and H. LÖWEN, *J. Phys.: Condens. Matter* **11**, 1435 (1999).
64. R. ROTH, private communication.
65. P. M. JOHNSON, C. M. VAN KATS, and A. VAN BLAADEREN, *Langmuir* **21**, 11510 (2005).
66. E. B. MOCK, H. DE BRUYN, B. S. HAWKETT, R. G. GILBERT, and C. F. ZUKOSKI, *Langmuir* **22**, 4037 (2006).
67. S. H. LEE, S. J. GERBODE, B. S. JOHN, A. K. WOLFGANG, F. A. ESCOBEDO, I. COHEN, and C. M. LIDDELL, *J. Mater. Chem.* **18**, 4912 (2008).
68. E. B. MOCK and C. F. ZUKOSKI, *Langmuir* **23**, 8760 (2007).
69. S. J. GERBODE, S. H. LEE, C. M. LIDDELL, and I. COHEN, *Phys. Rev. Lett.* **101**, 058302 (2008).
70. S. J. GERBODE, U. AGARWAL, D. C. ONG, C. M. LIDDELL, F. A. ESCOBEDO, and I. COHEN, *Phys. Rev. Lett.* **105**, 078301 (2010).
71. C. VEGA, E. P. A. PARAS, and P. A. MONSON, *J. Chem. Phys.* **96**, 9060 (1992).
72. C. VEGA, E. P. A. PARAS, and P. A. MONSON, *J. Chem. Phys.* **97**, 8543 (1992).
73. C. VEGA and P. A. MONSON, *J. Chem. Phys.* **107**, 2696 (1997).
74. C. VEGA, L. MACDOWELL, C. MCBRIDE, F. BLAS, A. GALINDO, and E. SANZ, *J. Mol. Liq.* **113**, 37 (2004).
75. M. MARECHAL and M. DIJKSTRA, *Phys. Rev. E* **77**, 061405 (2008).
76. T. BIBEN, R. OHNESORGE, and H. LÖWEN, *Europhys. Lett.* **28**, 665 (1994).
77. M. MARECHAL and M. DIJKSTRA, *Soft Matter* **7**, 1397 (2011).
78. L. ROSSI, S. SACANNA, W. T. M. IRVINE, P. M. CHAIKIN, D. J. PINE, and A. P. PHILIPSE, *Soft Matter* **7**, 4139 (2011).
79. S. HERNANDEZ-NAVARRO, P. TIERNO, J. IGNES-MULLOL, and F. SAGUES, *Soft Matter* **7**, 5109 (2011).
80. J. Y. KIM, F. E. OSTERLOH, H. HIRAMATSU, R. K. DUMAS, and K. LIU, *J. Phys. Chem. B* **109**, 11151 (2005).
81. J. A. CUESTA, *Phys. Rev. Lett.* **76**, 3742 (1996).
82. J. A. CUESTA and Y. MARTÍNEZ-RATÓN, *J. Chem. Phys.* **107**, 6379 (1997).
83. J. A. CUESTA and Y. MARTÍNEZ-RATÓN, *Phys. Rev. Lett.* **78**, 3681 (1997).
84. Y. MARTÍNEZ-RATÓN and J. A. CUESTA, *J. Chem. Phys.* **111**, 317 (1999).
85. F. SMALLENBURG, L. FILION, M. MARECHAL, and M. DIJKSTRA, *Proc. Natl. Acad. Sci. USA* **109**, 17886 (2012).
86. S. BELLI, M. DIJKSTRA, and R. VAN ROIJ, *J. Chem. Phys.* **137**, 124506 (2012).
87. J. H. CONWAY and S. TORQUATO, *Proc. Natl. Acad. Sci. USA* **103**, 10612 (2006).
88. Y. KALLUS, V. ELSER, and S. GRAVEL, *Discrete & Computational Geometry* **44**, 245 (2010).
89. E. CHEN, M. ENGEL, and S. GLOTZER, *Discrete & Computational Geometry* **44**, 253 (2010), 10.1007/s00454-010-9273-0.
90. A. JAOSHVILI, A. ESAKIA, M. PORRATI, and P. M. CHAIKIN, *Phys. Rev. Lett.* **104**, 185501 (2010).
91. S. TORQUATO, *Nature* **460**, 876 (2009).
92. J. DE GRAAF, R. VAN ROIJ, and M. DIJKSTRA, *Phys. Rev. Lett.* **107**, 155501 (2011).
93. S. TORQUATO and F. H. STILLINGER, *Rev. Mod. Phys.* **82**, 2633 (2010).
94. P. F. DAMASCENO, M. ENGEL, and S. C. GLOTZER, *Science* **337**, 453 (2012).
95. A. HAJI-AKBARI, M. ENGEL, A. S. KEYS, X. ZHENG, R. G. PETSCHKE, P. PALFFY-MUHORAY, and S. C. GLOTZER, *Nature* **462**, 773 (2009).
96. H. BRENNER, *J. Colloid Interface Sci.* **20**, 104 (1965).
97. H. BRENNER, *J. Colloid Interface Sci.* **23**, 407 (1967).

98. M. X. FERNANDES and J. GARCÍA DE LA TORRE, *Biophys. J.* **83**, 3039 (2002).
99. M. MAKINO and M. DOI, *J. Phys. Soc. Jpn.* **73**, 2739 (2004).
100. R. WITTKOWSKI and H. LÖWEN, *Phys. Rev. E* **85**, 021406 (2012).
101. D. J. KRAFT, R. WITTKOWSKI, B. TEN HAGEN, K. V. EDMOND, D. J. PINE, and H. LÖWEN, *submitted to Phys. Rev. Lett.* (2013).
102. A. HÄRTEL, R. BLAAK, and H. LÖWEN, *Phys. Rev. E* **81**, 051703 (2010).
103. S. VAN TEEFFELEN and H. LÖWEN, *Phys. Rev. E* **78**, 020101 (2008).
104. S. VAN TEEFFELEN, U. ZIMMERMANN, and H. LÖWEN, *Soft Matter* **5**, 4510 (2009).
105. B. TEN HAGEN, S. VAN TEEFFELEN, and H. LÖWEN, *J. Phys.: Condens. Matter* **23**, 194119 (2011).
106. M. POPESCU, S. DIETRICH, M. TASINKEVYCH, and J. RALSTON, *Eur. Phys. J. E* **31**, 351 (2010).
107. C. HOELL and H. LÖWEN, *Phys. Rev. E* **84**, 042903 (2011).
108. A. SENGUPTA, T. KRUPPA, and H. LÖWEN, *Phys. Rev. E* **83**, 031914 (2011).
109. H. H. WENSINK and H. LÖWEN, *Phys. Rev. E* **78**, 031409 (2008).
110. T. KIRCHHOFF, H. LÖWEN, and R. KLEIN, *Phys. Rev. E* **53**, 5011 (1996).
111. LÖWEN, H., *J. Chem. Phys.* **100**, 6738 (1994).
112. Y. YANG, V. MARCEAU, and G. GOMPPER, *Phys. Rev. E* **82**, 031904 (2010).
113. H. H. WENSINK and H. LÖWEN, *J. Phys.: Condens. Matter* **24**, 464130 (2012).
114. A. KAISER and H. LÖWEN, *Phys. Rev. E* **87**, 032712 (2013).
115. A. KAISER, H. H. WENSINK, and H. LÖWEN, *Phys. Rev. Lett.* **108**, 268307 (2012).
116. A. KAISER, K. POPOWA, H. H. WENSINK, and H. LÖWEN, *Phys. Rev. E* **88**, 022311 (2013).
117. J. BIALKÉ, T. SPECK, and H. LÖWEN, *Phys. Rev. Lett.* **108**, 168301 (2012).
118. A. M. MENZEL and H. LÖWEN, *Phys. Rev. Lett.* **110**, 055702 (2013).
119. M. SCHMIDT, *J. Phys.: Condens. Matter* **17**, S3481 (2005).
120. P. P. F. WESSELS, M. SCHMIDT, and H. LÖWEN, *Phys. Rev. Lett.* **94**, 078303 (2005).
121. M. REX and H. LÖWEN, *Phys. Rev. Lett.* **101**, 148302 (2008).
122. H. LÖWEN, *J. Phys.: Condens. Matter* **21**, 474203 (2009).